

Supporting Information – Shape and Phase Transitions in a PEGylated Phospholipid System

Lauri Viitala[†], Saija Pajari[†], Luigi Gentile^{‡,§,¶}, Jukka Määttä[†], Marta Gubitosi[‡], Jan Deska[†], Maria Sammalkorpi[†], Ulf Olsson[‡], Lasse Murtomäki^{†*}

[†] Department of Chemistry and Materials Science, Aalto University, P.O. Box 16100, FI-00076 Aalto, Finland

[‡] Physical Chemistry, Lund University, P.O. Box 124, SE-221 00 Lund, Sweden

[§] Department of Biology, MEMEG Unit, Lund University, Sölvegatan 37, SE-223 62 Lund, Sweden

[¶] Department of Chemistry, University of Bari Aldo Moro, Via Orabona 4, 70126 Bari, Italy

*Corresponding author: lasse.murtomaki@aalto.fi

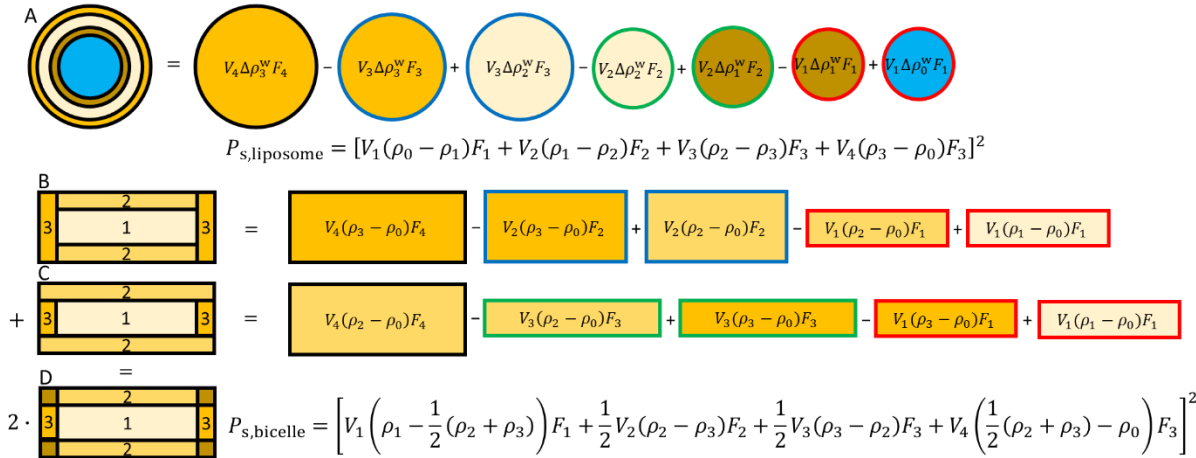
Contents

Small/Wide-Angle X-ray Scattering.....	S2
Core Shell Structure.....	S2
SAXS Fit Parameters	S3
WAXS Results.....	S4
Molecular Dynamics Simulations: additional details	S4
System Setup and Model Details in 10500 lipid systems.....	S4
Flat bilayer model.....	S5
Matlab Script for the Cryo-TEM Analyses	S6
References.....	S8

Small/Wide-Angle X-ray Scattering

Core Shell Structure

The core-shell structures of liposomes and bicelles are presented in Scheme 1. The entire structure is shown on the left and the component layers on the right. Each component layer i contains a factor $\pm V_i \Delta \rho_i^W F_i$, where V_i is its volume, F_i its form factor amplitude, and $\Delta \rho_i^W = \rho_i - \rho_0$ its scattering length density (SLD) in contrast with water (ρ_0 is the SLD of water).



Scheme 1. A: The core-shell structure of a liposome. On the left, the full representation; on the right, its divisions into component layers. B and C are two cylindrical core-shell structures with three layers (1, core; 2, face; and 3, rim). D represent a bicelle.

For a liposome (Scheme 1A), the component layers are 1) water, 2) the inner lipid head groups, 3) the lipid tail groups, and 4) the outer lipid head groups. These have spherical symmetry, characterized by the Rayleigh form factor amplitude¹ $F_i = 3(\sin qr_i - qr_i \cos qr_i)(qr_i)^{-3}$ that shows strong oscillation in the measurable q range. In a real system, polydispersity of the particles attenuates the oscillation. This can be taken into account with a Gaussian weight coefficient $I_j(\xi_j) = (\sqrt{2\pi} PDI \cdot r_1)^{-1} \exp(-\xi_j^2 (\sqrt{2} PDI \cdot r_1)^{-2})$, where PDI is the polydispersity index, r_1 is the radius of the water phase, and ξ_j is the deflection length that belongs to a group $\xi_j \in \{x | x \in \mathbb{R}, |x| \leq 3PDI \cdot r_1\}$. The idea is that each layer is deflected by ξ_j , so that $r_{i,j} = r_i + \xi_j$ and the volume is $V_{i,j} = \frac{4}{3}\pi r_{i,j}^3$. Hence,²⁻⁴

$$P_{s,\text{liposome}} = \sum_j I_j \left[\sum_i^4 \Delta \rho_i V_{i,j} 3 \frac{\sin qr_{i,j} - qr_{i,j} \cos qr_{i,j}}{(qr_{i,j})^3} \right]^2 = \sum_j I_j f_{i,j}^2, \quad (\text{S1})$$

where $\Delta \rho_i = \rho_{i-1} - \rho_i$ is the layer contrast with $\rho_4 = \rho_0$ and $\rho_1 = \rho_3$, because the lipid head groups are assumed self-similar.

The bicelle core was modelled as a combination of structures shown in Schemes 1B and 1C. The resulting structure is shown in Scheme 1D.

The form factor amplitude of a cylinder is given by Fournet⁵: $F_i = J_1(qr_i \sin \alpha) \sin(ql_i \cos \alpha) (q^2 r_i l_i \sin \alpha \cos \alpha)^{-1}$, where α is the angle between the incident beam and the cylinder normal, J_1 is the modified Bessel function of order 1, and l_i and r_i are the half-thickness and the radius of the i^{th} component layer. When the weighted polydispersity coefficient with the deflected radius $r_{i,j}$ and the volume $V_{i,j} = 4\pi r_{i,j}^2 l_i$ for each component layer are taken into account, the self-correlation term is

$$P_{s,\text{bicelle}} = \int \sum_j I_j \left(\sum_i^4 \Delta \rho_i V_{i,j} \frac{J_1(qr_{i,j} \sin \alpha) \sin(ql_i \cos \alpha)}{q^2 r_{i,j} l_i \sin \alpha \cos \alpha} \right)^2 \sin \alpha d\alpha = \int \sum_j I_j f_{b,j}^2 \sin \alpha d\alpha. \quad (\text{S2})$$

SAXS Fit Parameters

Table S1 shows the SAXS fit parameters used in the fit in Figure 2.

Table S1. SAXS fit parameters. The buffer scattering length density $\rho_0 = 0.95 \cdot 10^{11} \text{ cm}^{-2}$.

Liposomes					Bicelles				
x_{PEG}	0.03	0.06	0.12	-	x_{PEG}	0.12	0.15	0.24	-
R_{core}	33.56	32.55	27.80	[nm]	R_{core}	27.79	14.56	8.85	[nm]
d_{tail}	3.30	3.30	3.30	[nm]	d_{tail}	3.42	3.42	3.42	[nm]
t_{in}	1.05	1.11	1.11	[nm]	d_{face}	1.19	1.19	1.19	[nm]
t_{out}	0.97	0.97	0.97	[nm]	d_{rim}	0.45	0.45	0.45	[nm]
ρ_{tail}	0.87	0.87	0.87	[10^{11} cm^{-2}]	ρ_{core}	0.85	0.85	0.85	[10^{11} cm^{-2}]
ρ_{head}	1.17	1.17	1.17	[10^{11} cm^{-2}]	ρ_{face}	1.20	1.16	1.14	[10^{11} cm^{-2}]
					ρ_{rim}	1.04	1.04	1.04	[10^{11} cm^{-2}]
R_G	1.47	1.75	1.75	[nm]	R_G	1.75	1.92	1.92	[nm]
ρ_{PEG}	1.08	1.08	1.08	[10^{11} cm^{-2}]	ρ_{PEG}	1.08	1.08	1.08	[10^{11} cm^{-2}]
x_{out}	0.50	0.67	0.67	-	x_{rim}	0.20	0.44	0.43	-
PDI	0.40	0.45	0.25	-	PDI	0.25	0.25	0.25	-

x_{PEG}	PEG fraction
R_{core}	Core radius
d_{tail}	Lipid tail length
t_{in}	Head group layer thickness in the inner leaflet
t_{out}	Head group layer thickness in the outer leaflet
d_{face}	Head group layer thickness in the bicelle face region
d_{rim}	Head group layer thickness in the bicelle rim region
ρ_{tail}	Scattering length density of the lipid tail groups in liposomes
ρ_{head}	Scattering length density of the lipid head groups in liposomes
ρ_{core}	Scattering length density of the lipid tail groups in bicelles
ρ_{face}	Scattering length density of the lipid head groups in bicelle rim region
ρ_{rim}	Scattering length density of the lipid head groups in bicelle rim region
R_G	Radius of the gyration
ρ_{PEG}	Scattering length density of PEG
x_{out}	Fraction of PEG scattering on the outer leaflet
x_{rim}	Fraction of PEG scattering on the rim region
PDI	Polydispersity index

WAXS Results

Figure S1 presents the WAXS region of the SAXS/WAXS measurement of DPPC:DSPE-PEG with 3, 6, 12, 15 and 24 mol% of PEGylation at 25 °C, 41 °C and 50 °C.

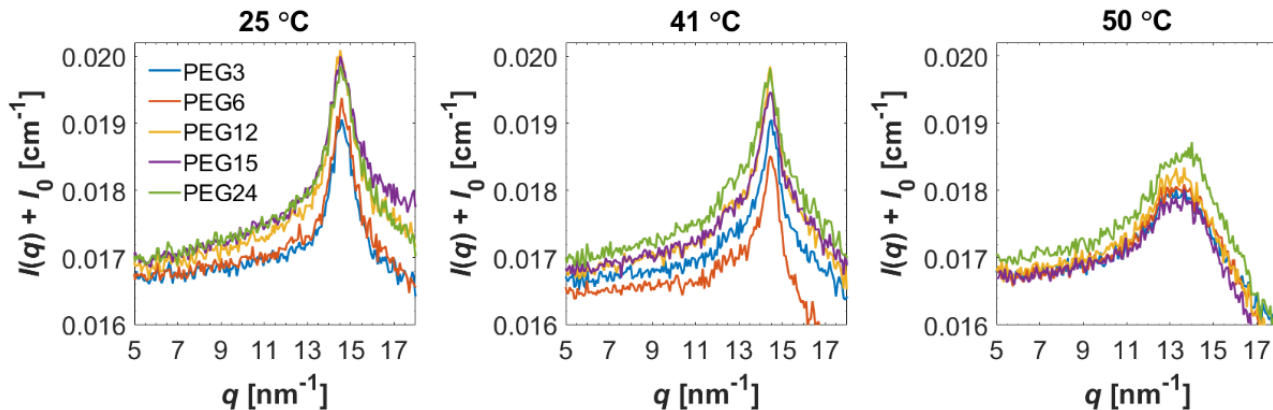


Figure S1. WAXS measurements of 3, 6, 12, 15 and 24 mol % PEGylated lipid samples at 25 °C, 41 °C, and 50 °C. I_0 is the average SAXS intensity of water ($1.641 \cdot 10^{-2} \text{ cm}^{-1}$).

Molecular Dynamics Simulations: additional details

System Setup and Model Details in 10500 lipid systems

For the DPPC and DSPE lipids, the DRY-MARTINI coarse-grained beads and parameters follow Ref. ⁶. The PEG chain is described by small DRY-MARTINI beads, called here SP_P and SP_h which represent a hydrated PEG monomer and the OH-termination in the PEG chain. For SP_P , each bead corresponds to a C-O-C unit. The DRY-MARTINI parameters of these beads are presented in Tables S2 and S3. The PEG chain linking to the DSPE lipid and the structures can be found in our earlier works.^{7,8}

Table S2. Parameters for the bonded interactions for the DRY-MARTINI polyethylene glycol (PEG) molecules. The X represents a bead linked to the PEG chain.

Bond or angle interaction	Equilibrium b [nm] or θ [degrees]	Force constant k_b [$\text{kJ mol}^{-1} \text{ nm}^{-2}$]	GROMACS interaction type
X- SP_P	0.41	3000	1
$\text{SP}_\text{P}-\text{SP}_\text{P}$	0.345	4500	1
$\text{SP}_\text{P}-\text{SP}_\text{h}$	0.33	4000	1
X-X- SP_P	180	35	2
$\text{SP}_\text{P}-\text{SP}_\text{P}-\text{SP}_\text{P}$	121	100	2
X- $\text{SP}_\text{P}-\text{SP}_\text{P}$	121	100	2
$\text{SP}_\text{P}-\text{SP}_\text{P}-\text{SP}_\text{h}$	121	100	2
CBT dihedral	Multiplicity n	Force constant a_n [kJ mol^{-1}]	GROMACS interaction type
$\text{SP}_\text{P}-\text{SP}_\text{P}-\text{SP}_\text{P}-\text{SP}_\text{P}/\text{SP}_\text{h}$	1	8.00	11
$\text{SP}_\text{P}-\text{SP}_\text{P}-\text{SP}_\text{P}-\text{SP}_\text{P}/\text{SP}_\text{h}$	2	1.21	11
$\text{SP}_\text{P}-\text{SP}_\text{P}-\text{SP}_\text{P}-\text{SP}_\text{P}/\text{SP}_\text{h}$	3	-1.85	11
$\text{SP}_\text{P}-\text{SP}_\text{P}-\text{SP}_\text{P}-\text{SP}_\text{P}/\text{SP}_\text{h}$	4	0.36	11
$\text{SP}_\text{P}-\text{SP}_\text{P}-\text{SP}_\text{P}-\text{SP}_\text{P}/\text{SP}_\text{h}$	5	0.76	11
$\text{SP}_\text{P}-\text{SP}_\text{P}-\text{SP}_\text{P}-\text{SP}_\text{P}/\text{SP}_\text{h}$	6	0.00	11

Table S3. Parameters for the non-bonded interactions for the DRY-MARTINI polyethylene glycol (PEG) beads and their interactions with the standard DRY-MARTINI lipid beads. The presented σ and ϵ are the Lennard-Jones parameters of the non-bonded interactions.

Bead pair	σ [nm]	ϵ [kJ mol ⁻¹]
SP _P SP _P	0.4300	0.3750
SP _h SP _P	0.4300	0.3750
SP _P SP _h	0.4300	0.3750
SP _h SP ₄	0.4300	2.0000
SP _h SP ₃	0.4300	2.0000
Q _{da} SP _P	0.4700	0.5000
Q _d SP _P	0.4700	0.5000
Q _a SP _P	0.4700	0.5000
Q ₀ SP _P	0.4700	0.5000
C ₃ SP _P	0.4700	2.3000
C ₁ SP _P	0.4700	1.8500
Q _{da} SP _h	0.4700	0.5000
Q _d SP _h	0.4700	0.5000
Q _a SP _h	0.4700	0.5000
Q ₀ SP _h	0.4700	0.5000
C ₃ SP _h	0.4700	1.0000
C ₁ SP _h	0.4700	0.5000

The bonded parameters (bonds, angles, torsions) have been obtained by fitting the resulting bond, angle, and dihedral distributions to reproduce the corresponding data sets obtained from atomistic simulations.^{9,10} Except for the torsions which use the CBT potential which enables longer simulation time step,¹¹ the bonded parameters correspond to harmonic functions. The non-bonded parameters, i.e. Lennard-Jones parameters, follow the octanol-water partition energies presented in Ref.⁶. The PEG self-interaction was tuned to reproduce PEG R₆ in solution, following Refs.^{9,12}. Following Wang and Larson¹³, the PEG-alkyl chain or lipid alkyl tail, i.e. PEG-C1 bead interaction is based on the free energy of pulling an 8 monomer long PEG chain (PEG₈) from a dodecane slab: the value $\epsilon = 1.85$ results in a well-depth of $-7.5k_B T$. Following procedures of Ref.¹², the parameters were validated by reproduction of short chain alkyl-ethoxylate C_nE_m phase diagrams.¹⁴

Flat bilayer model

To estimate the membrane thickness in the simulations, 100 ns simulations with pre-formed lamellar DPPC:DSPE-PEG bilayers were performed at 323 K temperature. These simulations consisted of 256 DPPC and 8 DSPE-PEG molecules (PEG3), 270 DPPC and 18 DSPE-PEG molecules (PEG6.25), and 144 DPPC and 18 DSPE-PEG molecules (PEG11.1) and estimate the bilayer thickness in zero curvature. A snapshot of PEG11.1 simulation is shown in Figure S2 on the left. The density profiles of lipid bilayers are shown on the right with the density profiles of the bicelle simulations consisting 1050 molecules (explained in the main text).

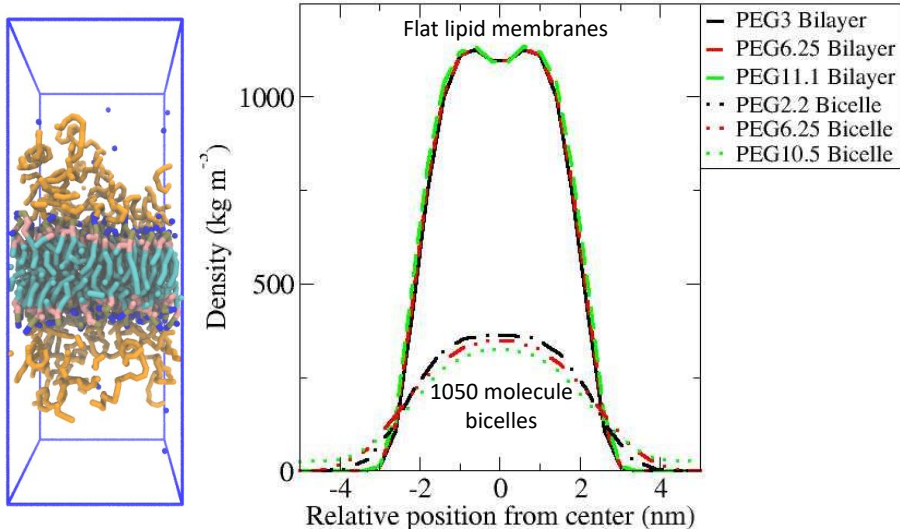


Figure S2. Left, snapshot of the PEG11.1 after 100 ns. Right, thickness of simulated flat lipid membranes and 1050 molecule bicelles (see the main text). Only the lipid density is shown; the PEG heads are omitted from the analysis. The thickness is estimated by full width at half maximum.

Matlab Script for the Cryo-TEM Analyses

This Matlab script is used to analyze cryo-TEM images. The script is used as follows: 1) run the script, 2) select the TEM image file(s), 3) click "Next Sample" to present the first image, 4) set the pixel size value according to your TEM image, 5) press "Add" to mark particulates, 6) adjust the zoom first and then click enter to start selecting particles; click the circumferential edges across the particle to obtain their size, 7) press enter when finished, 8) press "Remove" if you need to remove a miss-selection, 9) press "Save" to generate a txt data file, 10) press "Next Sample" to open the next TEM image; "Next Sample" displays a histogram if used for the last image.

```
function main()
% This function was written by Lauri Viitala (06/2017 in Helsinki,
% Finland). The function provides an user interface for the manual
% analysis of TEM data.
```

Selecting Images - multiselect on

```
close all
clear all
clc
global fc sizes centers size_st center_st fig p filename
fig = 0;
sizes = [];
centers = [];
size_st = [];
center_st = [];
%Selecting an image
[file,ruta] = uigetfile({'*.tif'; '*.bmp'; '*.xcf'}, 'Select a TEM image', 'Multiselect', 'on');
rut = cd(ruta);
filename = 'radius.mat';
if(iscell(file)==0)
    C{:}=cell2mat(num2cell(file));
    file = C;
end
p = length(file);
```

Controls/Buttons

```
pix0 = 0.851;% nm/pixel
h_next = uicontrol( 'Fontsize', 12.0, 'Position', [100 120 100 60], 'style', 'pushbutton', 'string', ' Next sample ', 'callback',
@next );
```

```

h_remove = uicontrol( 'Fontsize', 12.0, 'Position', [200 120 100 60], 'Style', 'pushbutton', 'String', ' Remove ', 'Callback',
@remove );
h_add = uicontrol( 'Fontsize', 12.0, 'Position', [300 120 100 60], 'Style', 'pushbutton', 'String', ' Add ', 'Callback',
@add );
h_save = uicontrol( 'Fontsize', 12.0, 'Position', [400 120 100 60], 'Style', 'pushbutton', 'String', ' Save ', 'Callback',
@savet );
);
h_pix_text = uicontrol( 'Fontsize', 12.0, 'Position', [100 300 100 60], 'Style', 'text', 'String', {' Pixel size [nm/pix] '} );
h_pixelsize = uicontrol( 'Fontsize', 12.0, 'Position', [100 270 100 30], 'Style', 'edit', 'String', num2str(pic0), 'callback',
@pixelsize );
function pixelsize(hObject, eventdata)
if ( hObject == h_pixelsize )
str = get( hObject, 'String' );
set( h_pixelsize, 'String', str );
end
function next(hObject, eventdata)
pix = str2num(get( h_pixelsize, 'String' ));
size_st = [size_st;sizes.*pix];
center_st = [center_st;centers];
sizes = [];
centers = [];
fig = fig+1;
if(p < fig)
figure();
hold on
hist(size_st,15);
xlabel('Diameter [nm]');
ylabel('Count')
cd(rut)
radius = size_st;
save(filename, 'radius');
else
fc = imread(file{fig}(:,:,1));
figure(2)
imshow(fc);
end
end
function remove(hObject, eventdata)
draw()
sel = 1;
while(sel==1)
figure(2)
[ai bi N] = ginput(1);
if(N==1)
[m ind] = min(sqrt((centers(:,1)-ai).^2+(centers(:,2)-bi).^2));
sizes(ind)=[];
centers(ind,:) = [];
else
sel = 0;
end
draw()
end
end
function add(hObject, eventdata)
draw()
sel = 1;
while(sel==1)
figure(2)
zoom on;
set(gcf, 'CurrentCharacter', char(14));
waitfor(gcf, 'CurrentCharacter', char(13))
[ai,bi,N] = ginput(2);
if(N==1)
r = 1/2*sqrt((ai(2)-ai(1)).^2+(bi(2)-bi(1)).^2);
center = [ai(1) bi(1)]+1/2*([ai(2) bi(2)]-[ai(1) bi(1)]);
sizes = [sizes;r];
centers = [centers;center];
else
sel = 0;
end
draw()
zoom reset
zoom off
end
end
function savet(hObject, eventdata)
klo = clock;
name = [num2str(klo(1)) '-' num2str(klo(2)) '-' num2str(klo(3)), ' ', num2str(klo(4)), '-' num2str(klo(5)), '-'
,num2str(round(klo(6))), '-' file{fig}, '.txt'];
pix = str2num(get( h_pixelsize, 'String' ));
center_st = [center_st;centers];
size_st = [size_st;sizes.*pix];
data = [center_st,size_st];
fileID = fopen(name, 'w');
del = '\t';
fprintf(fileID, ['x [pix]' ,del, 'y [pix]' ,del, 'radius [nm]' ,del,del,file{fig}]);
fprintf(fileID, '\r%f\t%f\t%f', data');
fclose(fileID);
end
function draw()
figure(2)
imshow(fc);
viscircles(centers, sizes, 'EdgeColor', 'r');
end
end

```

[Published with MATLAB® R2017a](#)

References

- (1) Lord Rayleigh, O. The Incidence of Light upon a Transparent Sphere of Dimensions Comparable with the Wave-Length. *Proc. R. Soc. Lond. A* **1910**, *84*, 25-46.
- (2) Pedersen, J. S.; Gerstenberg, M. C. Scattering Form Factor of Block Copolymer Micelles. *Macromolecules* **1996**, *29*, 1363-1365.
- (3) Kučerka, N.; Kiselev, M. A.; Balgavý, P. Determination of Bilayer Thickness and Lipid Surface Area in Unilamellar Dimyristoylphosphatidylcholine Vesicles from Small-Angle Neutron Scattering Curves: A Comparison of Evaluation Methods. *Eur. Biophys. J.* **2004**, *33*, 328-334.
- (4) Arleth, L.; Vermehren, C. An Analytical Model for the Small-Angle Scattering of Polyethylene Glycol-Modified Liposomes. *J. Appl. Cryst.* **2010**, *43*, 1084-1091.
- (5) Fournet, G. Scattering Functions for Geometrical Forms. *Bull. Soc. Fr. Min. Crist.* **1951**, *74*, 39-113.
- (6) Arnarez, C.; Uusitalo, J. J.; Masman, M. F.; Ingólfsson, H. I.; de Jong, D. H.; Melo, M. N.; Periole, X.; de Vries, A. H.; Marrink, S. J. Dry Martini, a Coarse-Grained Force Field for Lipid Membrane Simulations with Implicit Solvent. *J. Chem. Theory Comput.* **2015**, *11*, 260-275.
- (7) Aslan, S.; Määttä, J.; Haznedaroglu, B. Z.; Goodman, J. P.; Pfefferle, L. D.; Elimelech, M.; Pauthe, E.; Sammalkorpi, M.; Van Tassel, P. R. Carbon Nanotube Bundling: Influence on Layer-by-Layer Assembly and Antimicrobial Activity. *Soft Matter* **2013**, *9*, 2136-2144.
- (8) Määttä, J.; Vierros, S.; Van Tassel, P. R.; Sammalkorpi, M. Size-Selective, Noncovalent Dispersion of Carbon Nanotubes by PEGylated Lipids: A Coarse-Grained Molecular Dynamics Study. *J. Chem. Eng. Data* **2014**, *59*, 3080-3089.
- (9) Lee, H.; de Vries, A. H.; Marrink, S.; Pastor, R. W. A Coarse-Grained Model for Polyethylene Oxide and Polyethylene Glycol: Conformation and Hydrodynamics. *J. Phys. Chem. B* **2009**, *113*, 13186-13194.
- (10) Fuchs, P. F. J.; Hansen, H. S.; Hänenberger, P. H.; Horta, B. A. C. A GROMOS Parameter Set for Vicinal Diether Functions: Properties of Polyethyleneoxide and Polyethyleneglycol. *J. Chem. Theory Comput.* **2012**, *8*, 3943-3963.
- (11) Bulacu, M.; Goga, N.; Zhao, W.; Rossi, G.; Monticelli, L.; Periole, X.; Tielemans, D. P.; Marrink, S. J. Improved Angle Potentials for Coarse-Grained Molecular Dynamics Simulations. *J. Chem. Theory Comput.* **2013**, *9*, 3282-3292.
- (12) Rossi, G.; Fuchs, P.; Barnoud, J.; Monticelli, L. A Coarse-Grained MARTINI Model of Polyethylene Glycol and of Polyoxyethylene Alkyl Ether Surfactants. *J. Phys. Chem. B* **2012**, *116*, 14353-14362.
- (13) Wang, S.; Larson, R. G. A Coarse-Grained Implicit Solvent Model for Poly(Ethylene Oxide), CnEm Surfactants, and Hydrophobically End-Capped Poly(Ethylene Oxide) and its Application to Micelle Self-Assembly and Phase Behavior. *Macromolecules* **2015**, *48*, 7709-7718.
- (14) Mitchell, D. J.; Tiddy, G. J. T.; Waring, L.; Bostock, T.; McDonald, M. P. Phase Behaviour of Polyoxyethylene Surfactants with Water. Mesophase Structures and Partial Miscibility (Cloud Points). *J. Chem. Soc., Faraday Trans. 1* **1983**, *79*, 975-1000.